Direct imaging of molecular chains in a poly(*p*-xylylene) single crystal

Masaki Tsuji*, Seiji Isoda, Masayoshi Ohara, Akiyoshi Kawaguchi and Ken-ichi Katayama
Institute for Chemical Research, Kyoto University, Uji, Kyoto-Fu 611, *Japan*
(*Received* 3 *September* 1981)

Individual chains comprising a β-form poly(*p*-xylylene) (PPX) single crystal were resolved with a high resolution electron microscope (JEM-500). In a polymer crystal the important limiting factor for resolution is radiation damage. The total end point dose of a PPX crystal is about 0.5 coulomb cm^{-2} for 500 kV electron irradiation which is more than 20 times greater than that for a polyethylene crystal. The high resolution image obtained was processed by optical filtering to reduce noise due to the granularity of film. The processed image, which corresponds to the *ab*-plane projection of polymer chains, shows clearly the mutual arrangement of each molecule in the crystal. This high resolution image is sufficient to provide a starting point for determining the unknown crystal structure of the β-modification of PPX.

Keywords Poly(*p*-xylylene); high resolution electron microscopy; radiation damage; crystal structure; image processing; optical filtering

INTRODUCTION

Single crystals of various polymers have been studied by electron microscopy (EM). The application of EM has, however, been limited to the morphological investigation of polymer crystals and as such the molecular arrangement within a crystal has never been observed by EM, not only because the equipment did not have a sufficient resolving power to detect the individual molecular chains comprising the polymer crystals, but also because the polymer crystals are easily destroyed by electron irradiation. Consequently, one had to observe the specimens at low magnifications where a small amount of irradiation would be sufficient. In 1974, Kobayashi *et al.*[1] constructed a high resolution transmission electron microscope (TEM) (JEM-500). This TEM has a resolution of 0.15 nm and is able to give molecular or atomic images directly, only if the specimens are less radiation-sensitive.

Most polymer crystals are vulnerable to electron irradiation and are brought to an amorphous state by a small irradiation dose. Thus direct imaging of polymer molecules by EM is difficult practically. Only two studies have been done on one-dimensional lattice images of poly(*p*-phenylene terephthalamide)[2-4] and poly(*p*-xylylene) (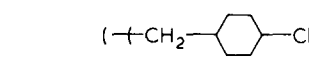 , PPX) crystals[5]. The locations of individual polymer chains comprising the polymer crystals have, up till now, never been realized. The fact that lattice images were obtained points to these polymers being seemingly less sensitive to electron irradiation. Therefore, for these polymers, it is highly probable that the molecular images would be obtained by high resolution EM. This is especially so with PPX as we can easily obtain a single crystal from solution.

The crystal structures of PPX were first reported in 1953 by Brown and Farthing[6] who discovered two crystalline modifications, α and β. In 1966, Niegisch[7] reported the morphologies of the α and β single crystals of PPX grown from α-chloronaphthalene solution. Kajiura *et al.*[8] have confirmed by X-ray measurements that these two types of single crystals correspond to the α- and β-modifications of the bulk materials observed by Brown and Farthing. The crystal structure of the α-form has already been analysed by Iwamoto and Wunderlich[9] but the crystal structure of the β-form is not yet known.

PREPARATION OF PPX SINGLE CRYSTALS

The PPX sample used was Parylene-N whose molecular weight is approximately 500 000 (Union Carbide Corp., U.S.A. provided through Tomoe Engineering Co. Ltd, Japan). After the Parylene-N film was dissolved in α-chloronaphthalene by heating at 254°C, the solution (0.05%) was held at 210°C overnight and then cooled to the room temperature. All treatments were performed under a nitrogen atmosphere to prevent polymer degradation due to the presence of oxygen. The polymer is also reported to be insoluble in the presence of oxygen[7]. Two entirely different types of single crystals developed from the solution under the experimental conditions described above. One is a rectangular crystal corresponding to the α-form (*Figure 1*) and the other a hexagonal crystal corresponding to the β-form (*Figure 2*). The crystal thickness of both the α- and β-forms was found to be about 10 nm from shadow length measurements. In the morphological study, electron images at a low magnification and selected area electron diffractions were all recorded on FUJI electron microscopic films (FG) with JEM-7A operating at 80 kV.

α-Form of PPX single crystal

In the case of the α-form of the PPX single crystal, two

* Present address: Department of Chemistry, Pulp and Paper Building, McGill University, Montreal, Canada

0032—3861/82/111568-07$03.00

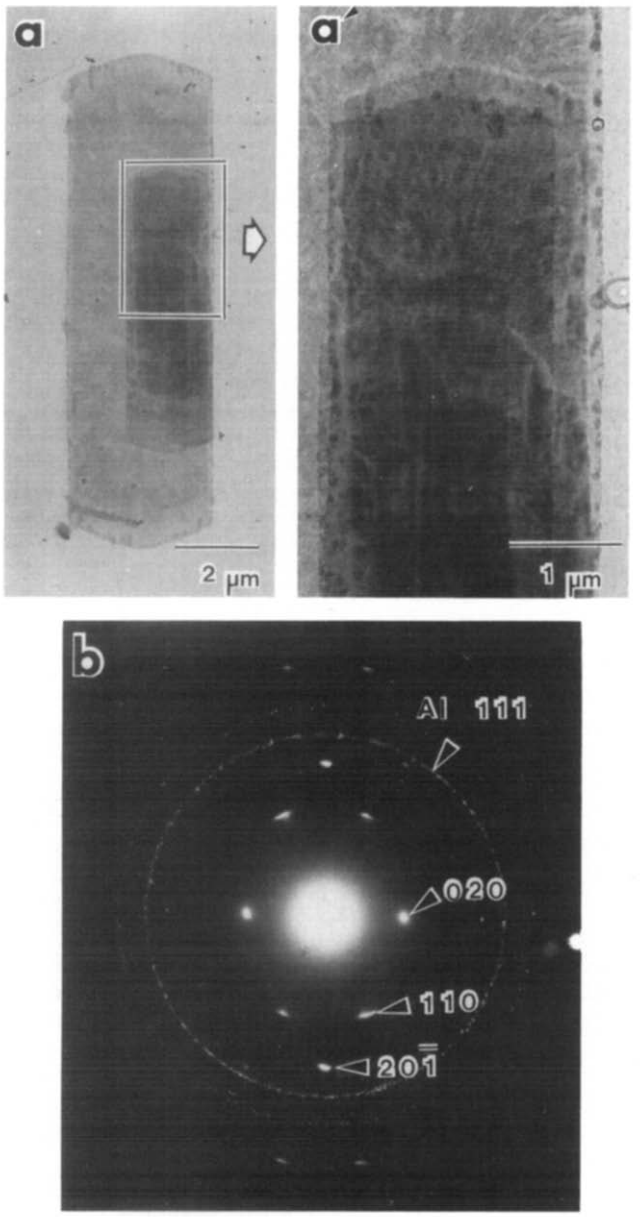

Figure 1 (a) PPX α-form single crystal. (a') Enlarged photograph of the enclosed part in (a). Moiré fringes are observed in the multi-layer part. (b) Electron diffraction pattern of an α-form single crystal on Al supporting film

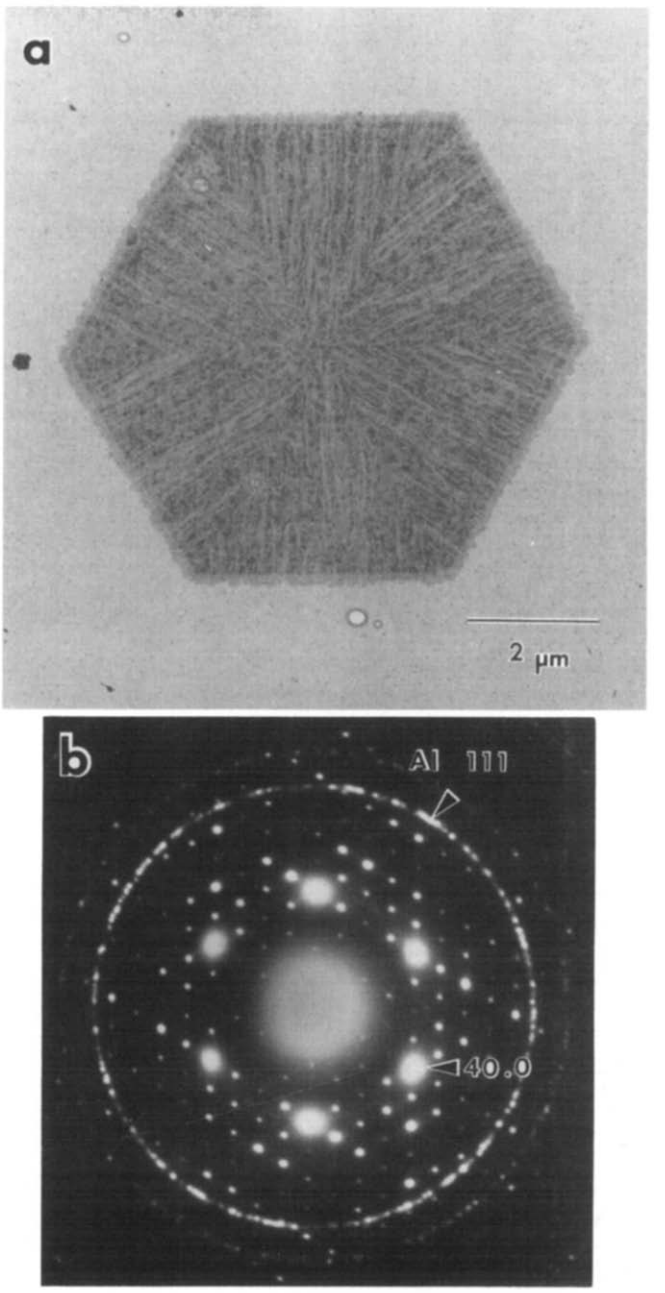

Figure 2 (a) PPX β-form single crystal. (b) Electron diffraction pattern of a β-form single crystal on Al supporting film

types of diffraction patterns were obtained, corresponding to the mono-layer and multi-layer crystals. *Figure 3* shows both kinds of selected area electron diffraction patterns and their double-exposed electron micrographs with a selected area aperture. As shown in *Figure 3a*, a basal mono-layer section yields the diffraction pattern attributed to the ⟨102⟩ incidence pattern only. A multi-layer section (*Figure 3b*) yields the 110 reflections attributed to the ⟨001⟩ incidence pattern and also the 20$\bar{1}$ reflection attributed to the ⟨102⟩ incidence pattern. Accordingly it is concluded that the chain axis in the basal mono-layer section is not perpendicular to the crystal end-surface, i.e., is not parallel to the direction of the incident electron beam. To the contrary, however, the chain axis in the overgrown layers is believed to be perpendicular to the crystal end-surface and parallel to the incident beam direction. The parallel fringes seen in the multi-layer section in *Figure 1a'* are Moiré image interference fringes. The weak radial striations observed

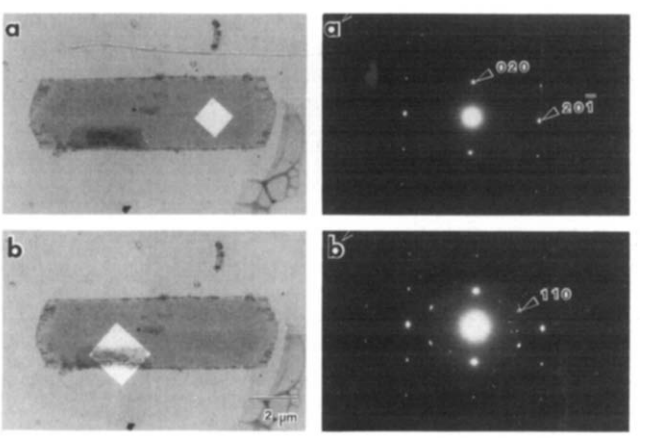

Figure 3 PPX α-form single crystals and corresponding selected area electron diffraction patterns. The squares in (a) and (b) show the selected area aperture positions corresponding to the diffraction patterns of (a') and (b'), respectively

in the basal layer are due to diffraction contrast, indicating that six sectors exist, as shown by a tent-like structure[10] prior to its deposition on the specimen supporting film. These fringes and striations are observed as long as the crystal is 'living' under electron irradiation.

β-Form of PPX single crystal

Most PPX β-form single crystals are hexagonal in shape as shown in *Figure 2*. The electron diffraction pattern of the β-form single crystal shows no systematic absence of reflections as reported by Niegisch[7] and has no symmetry planes. This diffraction pattern is characterized merely by the 6-fold rotational symmetry. These facts were confirmed by inspecting more than 100 photographs of the electron diffraction patterns of the β-form single crystals. The radial striations seen in *Figure 2* are due to a diffraction contrast as observed in the α-form, and they indicate that six (10.0) sectors exist in the β-form single crystal. All the sectors yielded identical diffraction patterns. The striations disappear under strong electron irradiation. Niegisch[7,11] has estimated the hexagonal unit cell dimensions ($a=2.052$ nm, c(molecular axis)$=0.658$ nm) and concluded that the molecules are all perpendicular to the single crystal end-surface.

SOME PROBLEMS IN DIRECT IMAGING OF MOLECULAR CHAINS IN A PPX SINGLE CRYSTAL

A resolution of 0.2 nm is the least required to obtain the information on the molecular arrangement in a polymer crystal. There are many factors which limit the resolution of TEM. In this section, the principal factors affecting the resolution of the individual chains comprising a single polymer crystal are summarized. As a result of following discussions, it becomes evident that the PPX β-form single crystal is quite suitable for the direct imaging of molecular chains.

Specimen thickness

In order to resolve a distance d_{min}, the specimen thickness must not exceed R_{max},

$$R_{max}=\frac{d_{min}^2}{2\lambda} \qquad (1)$$

from the standpoint of the Fresnel diffraction effect[12]. When $d_{min}=0.2$ nm and $\lambda=0.00142$ nm (the wavelength of a 500 keV electron), then R_{max} is estimated as 14 nm. The lamellar thicknesses of both the α- and β-form PPX single crystals is about 10 nm, i.e. less than R_{max}. Therefore a resolution of 0.2 nm, namely the resolution for individual polymer chains comprising the PPX single crystals, can be utilized where the above criteria are satisfied.

When the specimen is rather thick, then a dynamic scattering effect is introduced. Thus TEM images do not directly reflect the crystal structure (i.e. the projected potential distribution of the crystal) and their interpretation becomes more complicated. The extinction distance is one criterion for determining whether the diffraction behaviour of the electron is to be treated kinematically or dynamically[13]. The thickness of PPX single crystals is much smaller than half the extinction distance (about 160 nm) corresponding to the strong 40.0 reflection for 500 keV electrons. Therefore, the scattering of electrons through them can be treated kinematically.

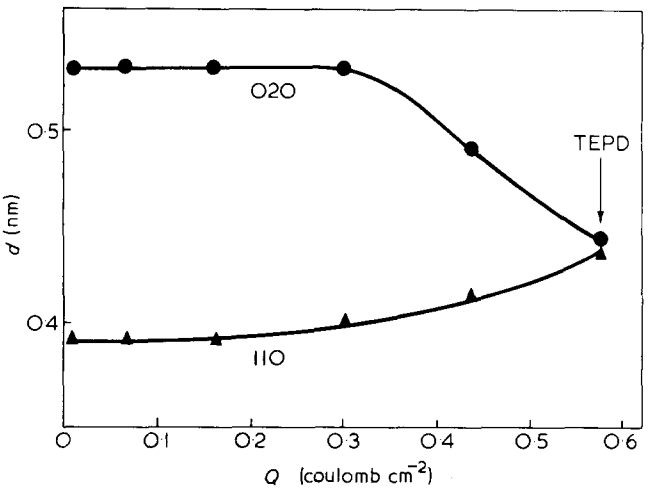

Figure 4 Lattice spacing changes of α-form single crystal due to electron irradiation; 110 reflection (▲) and 020 reflection (●). Spacings change sharply at 0.3 coulomb cm^{-2} and the crystal transforms to an amorphous state over 0.5 coulomb cm^{-2}

Specimen orientation

A high resolution image corresponds to a projection of potential along the electron beam direction in the kinematical study. If one hopes to obtain the atomic or molecular images from a crystal, one has to set correctly the particular direction of the crystal to the electron beam for the right superposition of atoms or molecules. A thin mono-layer crystal of the PPX α-form gives the selected area diffraction pattern attributed to the ⟨102⟩ incidence of electrons. The molecular axis of this crystal is not perpendicular to the crystal end-surface, but makes an angle 65° with the end-surface. Thus individual chains in this crystal cannot be expected to be resolved unless the specimen is inclined to the electron beam.

On the contrary, all the molecules align perpendicular to the crystal end-surface in a PPX β-form single crystal, so that the individual chains comprising this crystal can be resolved as the *ab*-plane projection of potential along the chain axis without specimen inclination.

Radiation damage of the specimen

The total end point dose (TEPD, the electron irradiation dose necessary for complete damage) for 500 keV electrons was about 0.5 coulomb cm^{-2} for both the α- and β-form PPX crystals, which is more than 20 times greater than that for polyethylene crystals (0.02 coulomb cm^{-2}). *Figure 4* shows the lattice spacing changes for 020 and 110 reflections of the α-form. The spacings do not change below 0.3 coulomb cm^{-2}. Above 0.3 coulomb cm^{-2}, both spacings drastically change and the crystalline reflections transform to an amorphous halo at about 0.5 coulomb cm^{-2}. The β-form (40.0) spacing increases slightly with electron dose as shown in *Figure 5* and the crystalline reflections also transform to an amorphous halo at about 0.5 coulomb cm^{-2}.

The resolution of the recording film is restricted to more than 20 μm due to the grain size of photographic film. In order to obtain the micrograph having a resolution of 0.2 nm, one must take photographs at a magnification (M) greater than 100 000. For Kodak electron image film SO-163, the exposure necessary for producing an optical density of 0.3 is about 2×10^{-11} coulomb cm^{-2} on the film. This exposure converts to ~0.2 coulomb cm^{-2} on a specimen at a magnification of 100 000 and is sufficiently

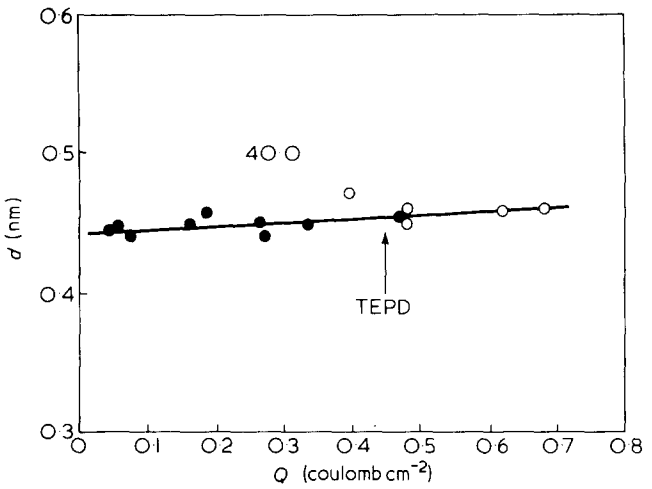

Figure 5 Lattice spacing changes of β-form single crystal due to 500 keV electron irradiation; crystalline 40.0 reflection (●), amorphous halo (○). The spacing slightly increases with electron dose and the crystal transforms to an amorphous state at about 0.5 coulomb cm^{-2}

lower than the TEPD. From the standpoints of radiation damage and photographic graininess, the magnification, in taking high resolution electron micrographs, was determined as $M = 100\,000$.

Specimen drift

In order to obtain high resolution electron micrographs, one should avoid the mechanical stage drift after specimen translation as well as the focus drift due to the magnetic hysteresis of the intermediate lens after a change-over from the diffraction mode to the imaging mode. Photographing should be postponed for several minutes, at least, to avoid these drifts. Electron exposure causes thermal deformation and charging of the specimen and the supporting film. They also create specimen drift and should be suppressed as carefully as possible.

A carbon- and gold-coated Triafol (cellulose acetobutyrate) microgrid (holey film) was used. A very thin carbon supporting film (produced by indirect evaporation onto a freshly cleaved surface of mica) was mounted on carbon- and gold-coated microgrids. This microgrid serves to increase the mechanical strength as well as the thermal and electrical conductivities. A carbon supporting film also suppresses the electron charging of the specimen. However, the carbon supporting film on the microgrid causes extra noise in the image. The monolayer single crystals of the β-form PPX are bent even on fairly small holes of the microgrid without a supporting carbon film, judging from irregular contours in the crystal due to diffraction contrast. To retain the correct orientation of the specimen, a carbon supporting film is required in spite of the noise disadvantage. A thin carbon film on the microgrid is considered to be the best supporting film to take a high resolution electron image.

Resolution limiting factors of electron microscope

In a high resolution study, a thin specimen should be used where the phase contrast is very important in the imaging of thin objects. The resolution of an electron microscope is determined by the phase contrast transfer function $\sin \chi(u)$. Here $\chi(u)$ is the phase retardation or the advance of the scattered electron and is expressed as,

$$\chi(u) = \pi\lambda\Delta f u^2 - \frac{\pi}{2} C_S \lambda^3 u^4, \qquad (2)$$

where u is the spatial frequency, λ the electron wave length, C_S the spherical aberration coefficient and Δf the defocus value[14]. In order to obtain an image which truly reflects the structure of the object, a high resolution electron micrograph should be taken under optimum focus conditions (Scherzer focus) that is determined by $\sin \chi(u)$. The phase contrast transfer functions for 500 keV electrons for various defocus values are shown in *Figure 6*. At 45 nm under focus the extended region of transfer function near unity is observed. Thus 45 nm under focus is estimated as the optimum defocus for JEM-500.

The illuminating angle and the energy spread of electrons deteriorate the resolution of the images. The phase contrast transfer function is multiplied by two envelope functions which are expressed in terms of the illuminating angle and the energy spread[15]. Although the two envelope functions considerably damp $\sin(\chi(u))$ to a smaller value for higher spatial frequency, these damping factors have no definite effect within a resolution of about 0.2 nm.

Astigmatism of objective lens

To obtain high resolution electron micrographs with resolution better than 0.2 nm the astigmatism of the objective lens must be compensated to within about 10 nm[16]. The detection of the image on the viewing screen of the high voltage TEM is too poor to permit us to compensate the astigmatism with such an accuracy. The accurate astigmatism correction method using optical transformation[17] was adopted in the present study.

Practically, no objective aperture was used. This was beneficial in avoiding the change of astigmatism due to

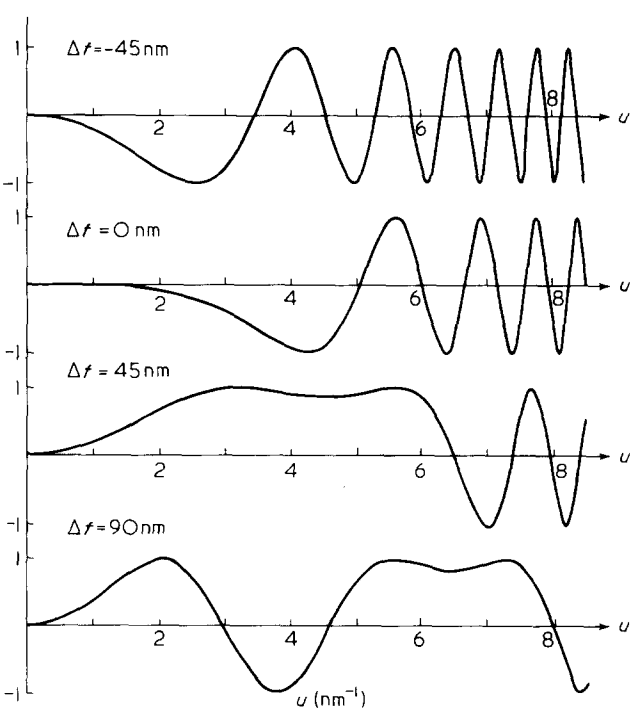

Figure 6 Phase contrast transfer function for 500 keV electrons. C_S is 1.06 mm. The extended region with amplitude near unity is observed at 45 nm under focus. The expected resolution is about 0.15 nm

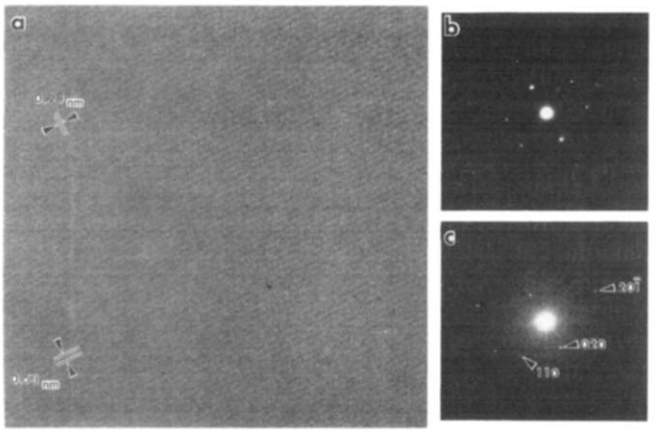

Figure 7 High resolution image of a PPX α-form single crystal. (a) High resolution electron micrograph. Fringes of 0.53 nm and 0.28 nm are observed and these correspond to (020) and (20$\bar{1}$) spacings. (b) Electron diffraction pattern taken at 500 kV. (c) Optical diffractogram of (a)

the deviation from the proper aperture position caused by frequent taking-in and -off of the aperture.

Recording systems

In high resolution transmission electron microscopy, the best medium for image recording now available is photographic emulsion. Although various recording devices[18,19] have been proposed for radiation-sensitive specimens, the resolution of these devices is generally inferior to that of photographic emulsion. Among various photographic films and plates, Kodak electron image films SO-163 were selected, because SO-163 is fairly good both in sensitivity and in resolution for 500 keV electrons.

PROCEDURES FOR TAKING HIGH RESOLUTION ELECTRON MICROGRAPHS

A high resolution EM (JEM-500) was used for taking a high resolution image of the PPX crystal. After the astigmatism of the objective lens was compensated for relative to specimen position, electron micrographs were taken at $M = 100000$ carefully avoiding radiation damage. The photographic films were developed at 20°C for 3 minutes with Kodak developer D-19 diluted 1:1 and fixed with Kodak rapid fixer. The micrographs obtained were analysed with an apparatus for an optical transformation which had already been constructed[20]. If the optical diffraction pattern from the micrograph resembles the electron diffraction pattern from the same specimen, it is judged that the micrograph reflects the true crystal structure of the specimen.

The resulting high resolution electron micrographs of both the α- and β-form PPX single crystals are shown in *Figures 7* and *8* with electron diffraction patterns and the optical diffraction patterns of the micrographs. The optical diffractogram (*Figure 7c*) reveals both the 110 and 20$\bar{1}$ reflections. This diffractogram shows that the micrograph (*Figure 7a*) was obtained at a multi-layer region of the α-form single crystal. Individual polymer chains of PPX of this α-form image were not resolved, because of the superposition of the two distinct crystal orientations. In the case of the β-form, the optical diffractogram (*Figure 8c*) closely resembles the electron diffraction pattern (*Figure 8b*) of ⟨00.1⟩ incidence. A similarity between the (*hk*.0) electron diffraction pattern (*Figure 8b*) of the β-form and the optical diffractogram (*Figure 8c*) of its high resolution micrograph (*Figure 8a*) indicates that the micrograph sufficiently reflects the crystal structure of the β-form. The diffractogram shows the reflections up to 44.0, the reflection corresponding to an interplanar spacing of 0.257 nm and such structure details should normally be recorded in the image. The structure details, however, cannot be recognized in this image, because of the low signal-to-noise (S/N) ratio due to the photographic graininess.

OPTICAL FILTERING OF THE HIGH RESOLUTION ELECTRON MICROGRAPH

To improve the S/N ratio of the high resolution electron micrograph of the PPX β-form single crystal (*Figure 8a*), optical filtering[21] was performed with a hexagonal filter grating (stainless steel plate; 30 mm in diameter and 0.2 mm thick, lattice constant 1 mm) having very small holes (100 μm in diameter). The schematic arrangement of pinholes in this filter is shown in *Figure 9*. In our experiments, only the holes which correspond to the sharp peaks in the diffractogram were used and the others were blocked. In this case, the hole size of the filter is so small

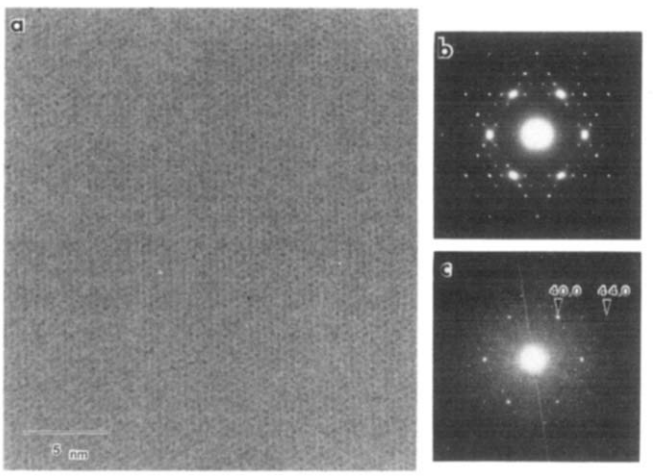

Figure 8 High resolution image of a PPX β-form single crystal. (a) High resolution electron micrograph. Individual molecules are roughly detectable as dark spots. (b) Electron diffraction pattern taken at 500 kV. (c) Optical diffractogram of (a)

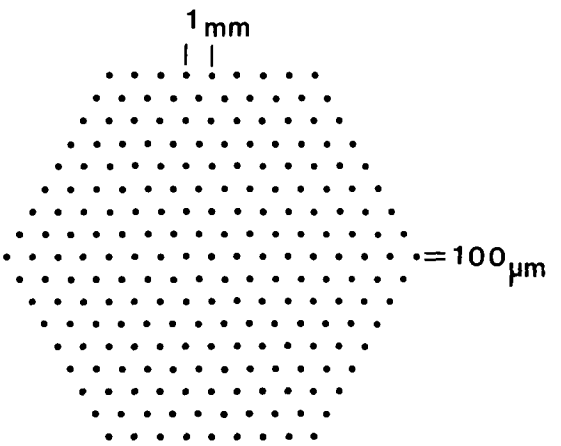

Figure 9 Schematic arrangement of pinholes in filter grating used for the optical image processing of the β-form high resolution micrograph

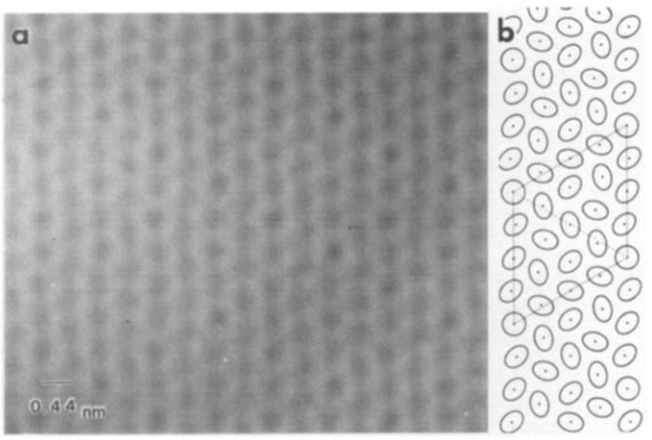

Figure 10 Processed high resolution image of a PPX β-form single crystal. (a) Optically filtered image using the filter grating shown in ***Figure 9***. (b) Model structure analysed by electron diffraction intensity

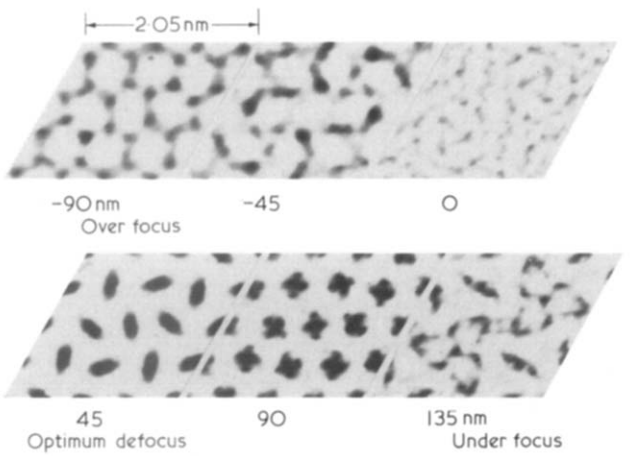

Figure 11 Simulated through-focal images to be taken with JEM-500; the wavelength 0.00142 nm, the spherical aberration coefficient 1.06 mm. Δf; the amount of defocusing (positive for under focus)

that effective averaging can be expected[22], and the periodicity in the image is emphasized. Processed images were recorded on Minicopy Film (a fine grain film, manufactured by Fuji Photo Film Co. Ltd., Japan) to avoid the quality degradation due to the granularity of the film, and the film was developed at 20°C for 6 minutes with Konidol Fine (manufactured by Konishiroku Photo Ind. Co. Ltd., Japan) which is used as a low contrast developer for Minicopy film. The processed image is shown in *Figure 10a*. From this figure, it is clear that reduction of random noise is achieved and details of the molecular arrangement are enhanced. Each black spot in this figure corresponds to a projected molecule along the polymer chain. This processed image clearly shows mutual positions of the chains in a unit cell projected on the *ab*-plane. It is shown that the chains are arranged in a wave pattern or zig-zag in the ⟨10.0⟩ directions. This gives a starting point for the structure analysis of the unknown β-form crystal. On the basis of this image, the crystal structure of the PPX β-form was analysed by the usual procedure using electron diffraction intensity and the result is shown schematically in *Figure 10b* where the molecule at the origin of a unit cell is represented by a circle and other molecules by ellipses to satisfy the P6 symmetry in the *ab*-plane projection. Detailed three-dimensional crystal structure analysis by X-ray diffraction was also performed, based on this processed image[23].

DISCUSSION

Molecular chains of PPX in the β-form single crystal were directly imaged with a JEM-500 microscope. This is the first case where molecular chains comprising a polymer crystal have been resolved.

Kobayashi says that 'seeing is not always believing at the resolution limit of electron microscope[24]. The image is greatly affected by the defocus value through $\sin \chi(u)$ in phase contrast electron microscopy[25]. Therefore, it is important to examine the consistency of the crystal structure of the objective specimen and the high resolution electron micrograph obtained. Usually this is done by comparing the obtained electron micrograph with through-focal images simulated from the crystal structure. Thus we simulated the through-focusing images to be taken with JEM-500. In the calculation with an electronic computer, the final structure parameters analysed by X-ray diffraction were assumed[23]. The computer simulation was performed according to the kinematical approximation using the following constants: the accelerating voltage 500 kV, the spherical aberration coefficient $C_s = 1.06$ mm and the maximum resolving power 0.15 nm. The results were displayed with a facsimile receiver[20] and are shown in *Figure 11*. This shows how greatly the high resolution electron microscopic image varies with the change in defocus (Δf). The simulated image at 45 nm under focus (optimum focus) resembles the micrograph actually obtained. This computer-simulation confirms that the obtained micrograph (*Figure 10a*) does not contradict the results from the crystal structure analysis by X-ray diffraction. Moreover, this shows that one cannot expect to resolve up to the individual carbon atoms in a PPX molecule in the *ab*-plane projection, because the atoms in the molecule are close together in the projection.

For the image of the α-form, optical filtering was also performed and the image obtained was compared with the computer simulated images where the incidence of electrons is in the ⟨102⟩ direction. The simulation clearly shows that the molecular structure cannot be seen in this incident direction and there is no inconsistency between the processed and simulated images.

ACKNOWLEDGEMENTS

The authors would like to acknowledge Dr Kazuo Ishizuka for his permission to use his computer program for kinematical image-simulation, and Tomoe Engineering Co. Ltd., Japan, for the supply of a PPX specimen (Parylene-N).

REFERENCES

1 Kobayashi, K., Suito, E., Uyeda, N., Watanabe, M., Yanaka, T., Etoh, T., Watanabe, H. and Moriguchi, M. Proceedings of 8th International Congress on Electron Microscopy, Canberra, 1974, **1**, 30

2 Dobb, M. G., Hindeleh, A. M., Johnson, D. J. and Saville, B. P. *Nature* 1975, **253**, 189

3 Bennett, S. C., Dobb, M. G., Johnson, D. J., Murray, R. and

Saville, B. P. Proceedings of Electron Microscopy and Analysis Group, Bristol, 1976, 329
4 Dobb, M. G., Johnson, D. J. and Saville, B. P. *J. Polym. Sci., Polym. Symp. Edn.* 1977, **58**, 237
5 Bassett, G. A. and Keller, A.; cited by Keller, A. *Kolloid-Z.* 1969, **231**, 386
6 Brown, C. J. and Farthing, A. C. *J. Chem. Soc.* 1953, **1953**, 3270
7 Niegisch, W. D. *J. Appl. Phys.* 1966, **37**, 4041
8 Kajiura, A., Fujii, M., Kikuchi, K., Irie, S. and Watase, H. *Kolloid-Z.* 1968, **224**, 124
9 Iwamoto, R. and Wunderlich, B. *J. Polym. Sci., Polym. Phys. Edn.* 1973, **11**, 2403
10 Kubo, S. and Wunderlich, B. *Makromol. Chem.* 1972, **162**, 1
11 Niegisch, W. D. *J. Appl. Phys.* 1967, **38**, 4110
12 Cowley, J. M. 'Diffraction Physics', Chapter 13, North-Holland, 1975
13 Hirsch, P. B., Howie, A., Nicholson, R. B., Pashley, D. W. and Whelan, M. J. 'Electron Microscopy of Thin Crystals', Chapter 4, Butterworths, 1965
14 Scherzer, O. *J. Appl. Phys.* 1949, **20**, 20
15 Wade, R. H. and Frank, J. *Optik* 1977, **49**, 81
16 Kobayashi, K. and Uyeda, N. Proceedings of 8th International Congress on Electron Microscopy, Canberra, 1974, **1**, 264
17 Krivanek, O. L., Isoda, S. and Kobayashi, K. *J. Microscopy* 1977, **111**, 279
18 Thomas, E. L. and Ast, D. G. *Polymer* 1974, **15**, 37
19 Catto, C. J. D. and Smith, K. C. A. *J. Microscopy* 1975, **105**, 223
20 Tsuji, M., Isoda, S., Ohara, M., Katayama, K. and Kobayashi, K. *Bulletin of the Institute for Chemical Research, Kyoto Univ.*, 1977, **55**, 237
21 Klug, A. and DeRosir, D. J. *Nature* 1966, **212**, 29
22 Aebi, U., Smith, P. R., Dubochet, J., Henry, C. and Kellenberger, E. *J. Supramol. Structure* 1974, **1**, 498
23 Isoda, S. *et al.*, to be submitted
24 Kobayashi, K. Proceedings of Electron Microscopy and Analysis Group, Bristol, 1976, 251
25 Ishizuka, K. and Uyeda, N. *Bulletin of the Institute for Chemical Research, Kyoto Univ.* 1975, **53**, 200